Korean J. Chem. Eng., **31**(4), 541-547 (2014)
DOI: 10.1007/s11814-014-0050-2
pISSN: 0256-1115
eISSN: 1975-7220

INVITED REVIEW PAPER

Lithographically patterned micro-/nanostructures via colloidal lithography

Jin Young Park†

Department of Polymer Science and Engineering, Kyungpook National University,
80, Daehak-ro, Buk-gu, Daegu 702-701, Korea
(*Received 23 December 2013 • accepted 8 February 2014*)

Abstract−Colloidal lithography is an effective and facile strategy for highly ordered nanostructure arrays that is a simple, inexpensive, and high-throughput process with a broad choice of materials in manufacturing various lithographically patterned nanostructures on substrates. To develop such nanostructured systems, various nanofabrication techniques are employed on two-dimensional (2D) colloidal masks for evaporation, electrochemical deposition, etching, dewetting and mask replication. Ordered nanostructures associated with feature shapes and sizes can be diversified through a choice of methodology and a control of experimental conditions. This review presents an overview of colloidal crystals as a mask and nanostructure arrays (nanopillars, nanoring, nanopores) fabricated by colloidal lithography as well as introducing practical applications using ordered nanostructures.

Keywords: Colloidal Crystal, Colloidal Lithography, Nanostructure, Nanopillar, Nanopore

INTRODUCTION

Monodisperse microspheres, such as polystyrene (PS), poly(methyl methacrylate) (PMMA) or silica (SiO_2), self-assembled with a hexagonal close-packing (hcp) array can be successfully driven using numerous technologies related to colloidal crystallization including solvent evaporation [1-4], vertical deposition [5], dip-coating [6], spin-coating [7,8], spin-coating and floating-transfer [9,10], template-assisted growth [11,12], depletion force induced crystallization [13], and Langmuir-Blodgett-like transfer method [14-16]. As lithographic tools, self-assembled hcp solid sphere arrays can be used in order that specific nanomaterials are grown from interstices existing among close-packed colloids during deposition. In general, quasi-triangular nano-objects are arranged with P6mm symmetry on a substrate from a single colloidal layer after deposition and the removal of a mask. Various types of deposition methods (typically, e.g., chemical vapor deposition or electrochemical deposition) have been effectively used to grow nanomaterials such as polymers [17,18], metals [19], or inorganic materials [20]. As a more advanced lithographic approach, non-close packed (ncp) arrays have recently been used as masks to accomplish lithographically structured nanopillar, nanopore, nanoring formation [21] as well as for further nanostructure designs (e.g. binary/ternary hybrid particles [22] and polymer pillars) [23].

For patterned polymer brushes (bottom-up approach), numerous lithographic methodologies were systematically combined such as photo-/interface lithography, electron-beam lithography, scanning probe lithography, soft lithography, and other lithographic approaches [24]. In particular, colloidal lithography has broad potential availability for polymer brush due to relatively low cost colloids and simple preparation to create micro-/nanopatterned templates compared to other lithographic approaches. In addition, it allows polymer brush geometry to be controlled by simply changing the diameter or chemical functionality of the nano/microspheres. In this regard, many studies have been performed using colloidal lithography, such as poly(4-vinylpyridine)-*block*-poly(4-iodo-styrene), [P4VP-b-PS(I)] adsorbed selectively onto hydrophilic spots [25], hole shaped patterned polymer brushes [poly(*n*-isopropylacrylamide); PNIPAAM] grown on 11-(2-bromo-2-methyl)propionyloxy) undecyltrichlorosilane via surface-initiated atom transfer radical polymerization (SI-ATRP) [26], cone-shaped PNIPAAM brushes grown from initiator templates patterned via self-assembled microsphere monolayers used directly as stamps for microcontact printing (m-CP) [27], stimulus-sensitive PNIPAAM polymer brushes via temperature grating [28].

Furthermore, using colloidal crystal templates in combination with chemical vapor deposition (CVD) [29,30], glancing angle deposition (GLAD) [31] or etching of colloidal crystals prior to metal deposition (for ncp arrays) [32], various nanoporous structures have been developed for chemical analysis and characterization [33,34] including an optical phenomenon [35], photosensitive devices (e.g. wavelength-selective photoswitches) [36], sensing templates to analyze chemical/biological materials [37,38], and optoelectronic devices [39]. Thus, focusing on new lithographic techniques developed for last five years (2009-2013), the fabrication methodologies and applications of nanostructured arrays prepared using colloidal lithography are discussed in this article.

COLLOIDAL CRYSTALS

Recently, a novel attractive force gradient method was introduced for a perfect, single-domain 2D colloidal crystal [40]. In a water-lutidine binary liquid mixture, a well-controlled attractive force gradient arises from a temperature gradient. Specifically, nucleation of colloidal crystals in the mixture preferably occurs in a high temperature region because of relatively stronger attraction, and crystallization propagates from the high temperature region to the low tem-

†To whom correspondence should be addressed.
E-mail: jinpark@knu.ac.kr

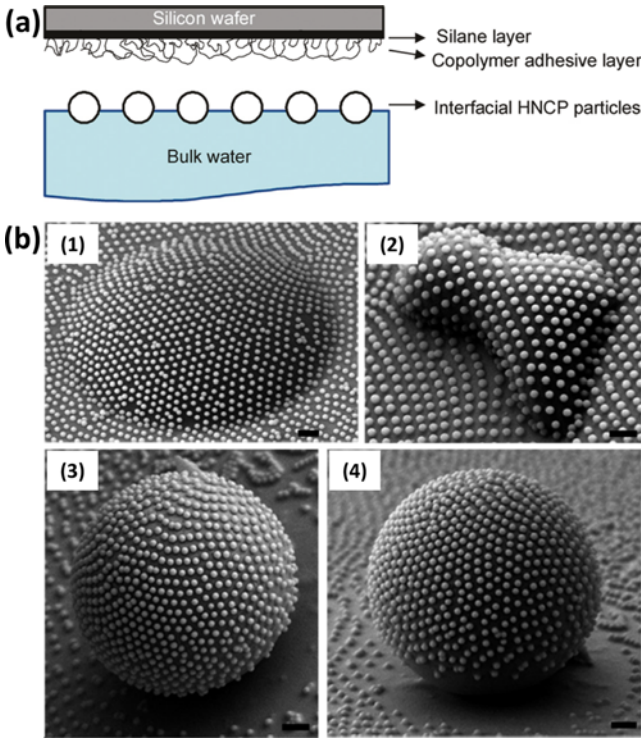

Fig. 1. (a) Schematic illustration of transferring interfacial HNCP particle arrays and (b) distorted HNCP arrays of 370 nm particles coated on a spherical mound (1), an irregularly shaped mound (2), and a 10 μm latex sphere (3: top view and 4: side view). Scale bar: 1 μm. Reprinted with permission from Ref. 44. Copyright 2010 American Chemical Society.

perature region in a well-controlled way. This effective method may provide 2D hcp colloidal crystal for further applications such as photonic crystal and colloidal lithography.

In addition, using hcp SiO_2 microsphere arrays, 2D periodic ncp colloidal arrays with tunable lattice spacing, lattice structure, and pattern arrangement were fabricated by a combination of soft lithography and controlled deformation of polydimethylsiloxane (PDMS) elastomer [41]. The lattice spacing and lattice structure in 2D hcp microsphere arrays transferred on the surface of PDMS stamps can easily be adjusted by solvent swelling or mechanical stretching of the stamps. The PDMS assisted deformation strategy gives rise to various lattice features, possibly used as molds for porous films or nanowires. Along with the mechanical deformation, a reactive ion etching (RIE) process can be used on transferred SiO_2 or PS particles to generate ncp arrays [42], and the arrays are sequentially transferred on PDMS molds [43]. For ncp arrays on nonplanar surfaces, Jia et al. reported that interfacial hexagonal noncontiguously packed (HNCP) PS particles on bulk water can be transferred onto copolymer/silane adhesive bilayered substrates (Fig. 1) [44]. Similarly, polymer brushes [poly(*n*-butyl acrylate) and poly(*n*-butyl acrylate-*random*-*N*,*N*-diethylaminoethyl acrylate)] grafted via ATRP (a "graft-from" method) can be used as adhesive promoters for a hexagonal lattice [45].

COLLOIDAL LITHOGRAPHY

1. Patterned Self-assembled Monolayers and Polymer Brushes

Colloidal lithography can be used to fabricate patterned self-assembly monolayers (*p*-SAM) as masks [46] or patterned polymer

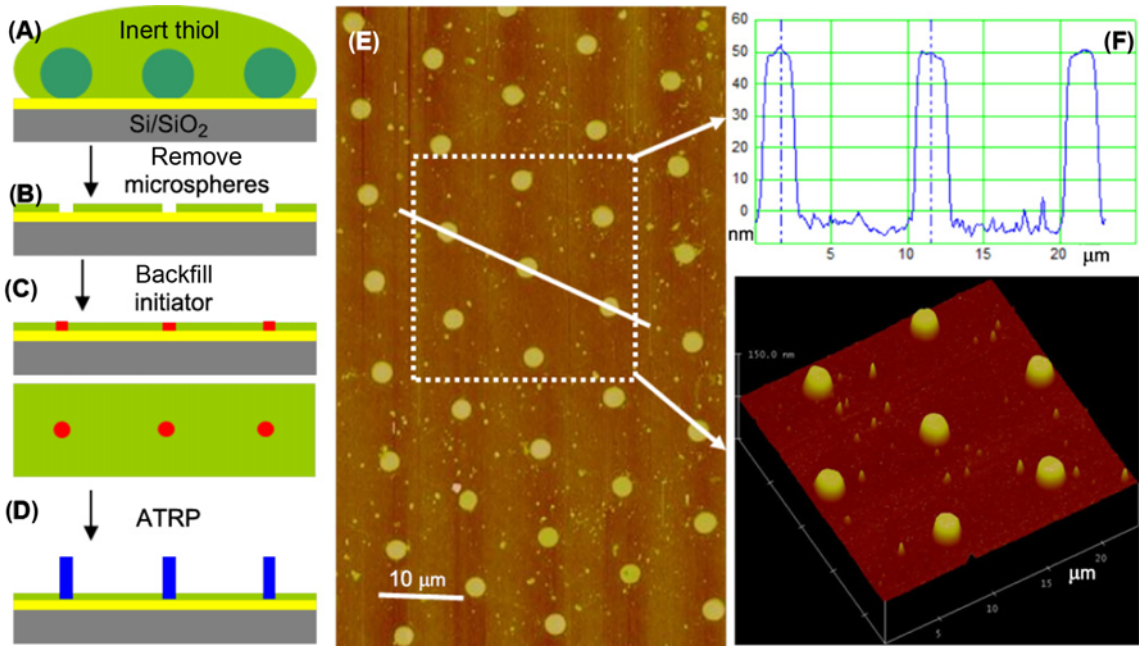

Fig. 2. Schematic illustration and AFM images for patterning polymer-brush pillars through the use of colloidal lithography. (A) An ncp array on a gold substrate served as a mask for an inert thiol SAM pattern. (B) The inert thiol SAM pattern formed after the ink transfer and the removal of the colloidal array. (C) A thiol initiator backfilled on the patterned substrate. (D) Polymer-brush microstructure formed by SI-ATRP of NIPAAM. (E) AFM height images (contact-mode) of the patterned PNIPAAM-brush microstructure and (F) the corresponding height profiles and 3-D image. Reprinted with permission from Ref. 47. Copyright 2012 Beilstein Journal of Nanotechnology.

cylinders via an inert thiol SAM formation on ncp colloidal arrays and sequential polymer brush synthesis (SI-ATRP of NIPAAM) on periodic spots formed after mask removal (Fig. 2) [47]. Moreover, Gleason and coworkers introduced a combination method of colloidal lithography and initiated chemical vapor deposition (iCVD) as a bottom-up approach to graft various polymers such as organic polymers, fluoropolymers, and organosilicones on vinyl groups-modified exposed regions of a hcp colloidal mask [29,30]. As mentioned above, *p*-SAM or polymer brushes formed by lithographic tools are highly important for array-based platforms and applications in surface-based technologies, such as protein resistant or adsorbed coatings and substrates for cell-growth control or separation of biological molecules. As one example, Yang and coworkers demonstrated protein patterns [human immunoglobulin G (IgG)] covalently immobilized on hierarchical poly(2-hydroxyethyl methacrylate) (PHEMA) brush via colloidal lithography, photolithography, and two-step colloidal lithography [48]. In this process, the formation of various protein patterns (microdiscs, microstripes, microrings, microtriangles, and microgrids) depends upon tunable parameters of protein patterns, such as height, diameters, periods, and distances between two dots.

2. Nanopillars

In most instances, well-ordered periodic nanopillars can be generated using colloidal lithography and dry etching techniques (inductively coupled plasma or reactive ion etching). Recently, various inorganic materials such as GaAs [49], InP [50], and Si [51-54] were used to fabricate nanorod or cone arrays. These well-defined patterns on substrates are of considerable interest as a potential technology for applications ranging from basic research to biosensors and bioMEMS. Tserepi and coworkers [55] demonstrated a low-cost and high throughput process for nanoscale, selective immobilization of proteins (streptavidin) on biotinylated bovine serum albumin (*b*-BSA)-adsorbed SiO_2 patterned spots, based on colloidal lithography and plasma processing.

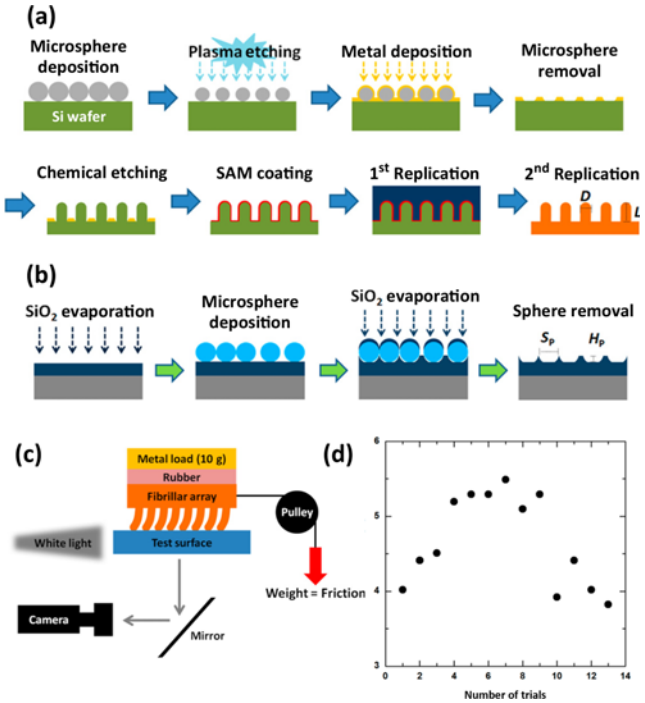

Fig. 3. A procedure for (a) LDPE fibrillar array fabrication and (b) a patterned rough counter-surface. (c) An example of friction tests for one fibrillar array sample. Reprinted with permission from Ref. 32. Copyright 2012 American Chemical Society.

Furthermore, polymeric nanofibers were also arranged using colloidal lithography and mask replication (Si template) methods for a study of friction characteristics (Fig. 3) [32,56]. Ordered low-density polyethylene (LDPE) nanofiber arrays with various asperity heights, spacings, and area fractions were replicated from Si nanowire, and friction behaviors between fibrillar arrays and rough surfaces were observed in independent control of several major parameters for characterizing a rough surface. This study provided meaningful insights on what important parameters are required in designing an adhesive, related to friction behaviors. Another method to manufacture nanopillars is to use a polymer layer (e.g., PMMA) spun-coated on a substrate prior to colloidal arrangement. Gogolides and coworkers [57,58] developed large-area, unform, ordered PMMA nanopillars using so-called "mesh-assisted" colloidal lithography and plasma nanotexturing. In a similar manner, Au islands were fabricated on top of PMMA pillars on glass substrates using PMMA/gold bilayers through a simple and versatile colloidal lithography method for an improvement of refractive index sensitivity of localized surface plasmon resonance (SPR) sensors [59].

3. Other 2D and 3D Structures

In general, colloidal crystals have been used as a mask to fabricate porous structured arrays such as nanoholes [35,60,61], periodically serrated strips arrays [62], and 2D thin [63] or binary [64] porous arrays. However, this lithographic approach is extendable to an inverted porous polymer [65] or hemispherical [66] mask fabrication for further applications. In this section, various nanostructures such as materials-based nanopores, nanoring, and hollow spheres are described focusing on fabrication methodologies.

3-1. Metals/Magnetic Materials

In contrast to the use of colloidal particles applied as a mask in colloidal lithography, thermal decomposition of metal-covered particles was employed to precisely produce metal structures [67]. Large arrays of metal (Au, Ag, Pt) nanoparticles can be produced as follows: (i) Convectively assembled hcp PS arrays are coated with a metal and (ii) annealed in a resistive furnace or using an ethanol flame. (iii) Through the thermal decomposition, the metal layer is converted into particles arranged in hexagonal arrays that retain the order of the original monolayer. In this case, both the particle size and the interparticle distance can be adjusted by the thickness of the coated metal and the sphere diameter, respectively. As an inverse approach, a protocol combining colloidal lithography, metallization and template stripping was reported by Albrektsen and coworkers [68]. Au films with inter-connected nanostructures consisting of either partial spherical shells or inverted structures (spherical cavities) were constructed, and the nanocavities showed distinct sensitivity with respect to the refractive index of the cavity, potentially for use as imprinted cavities for sensing devices. Furthermore, homogeneously distributed pair nanodisks (Pt and Ru) were prepared using hole-mask colloidal lithography to investigate the effects of bimetallic catalyst electrodes on electrocatalytic reactions [69], and for magnetic nano-scaled structures, various magnetic materials such

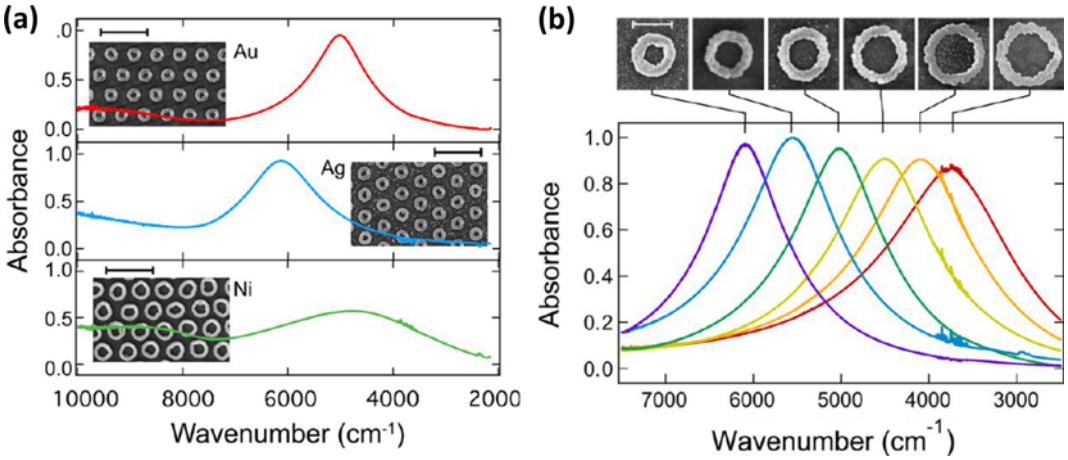

Fig. 4. NIR spectra of (a) Au, Ag, and Ni nanoring arrays showing plasmonic resonances in the near-infrared and corresponding SEM images (scale bar=2 mm) and (b) Au ring resonance with varying radius (each spectrum is shown with its corresponding SEM of a single nanoring from the array) (scale bar=500 nm). Reprinted with permission from Ref. 72. Copyright 2013 American Chemical Society.

as thin Fe films [70], or Co/Pt multilayers [71] on ncp arrays were used.

3-2. Nanorings

Another approach of colloidal lithography yields nanorings via metal deposition on colloidal arrays and sequential etching process. Nanoring array, consisting of three plasmonic metals (Au, Ag, and Ni), was fabricated via a combination process of lithographically patterned nanoscale electrodeposition (LPNE) and colloidal lithography (Fig. 4) [72]. These nanoring arrays exhibited a change in a single strong near-infrared (NIR) plasmonic resonance depending on the radius and width of the arrays. In addition, it was possible to create more complex concentric ring structures with multiple NIR plasmonic resonances. Thus, this method may be applied to other LPNE compatible metals, semiconductors, and conductive polymers for nanoring array formation. For highly tunable and multiple plasmonic resonances, another methodology was introduced to form elliptical metal nanorings by the following steps [73]: (i) hexagonally arrayed PS rings were used as masters to generate PDMS stamps with circular apertures. (ii) The stretched stamps were then used as molds to create elliptical PS rings by a capillary filling process. (iii) Going through subsequent RIE and chemical wet etching, the elliptical PS rings were readily transferred onto an underlying Au film, finally resulting in the formation of Au nanorings. The aspect ratio of the resultant elliptical nanorings could controllably tune resonant modes across a broad spectral range from the visible to the mid infrared.

In addition, plasmon hybridization observed in stacked double crescents arrays, consisting of Au and SiO_2/Au, fabricated via evaporation and RIE etching process was studied by Butt and coworkers [74]. In the close proximity of the nanocrescents, a coupling process generated new optical resonances due to linear superposition of plasmonic modes that occurred from individual crescents. Similarly, Si or Au crescent nanoring arrays were also studied, made by angle depositing on individual particles (ncp arrays) as shadow masks [75]. More interestingly, Yang and coworkers reported how to fabricate poly(vinyl alcohol):rhodamine B (PVA:RB)/poly(N-vinylcarbazole (PVK) heterogeneous double-ring-like (HDR) structure arrays using controllable dewetting on 2D ncp SiO_2 sphere arrays, which is extendable toward potential application in optoelectronic devices, surface photocatalysis, and surface enhanced Raman scattering (SERS) (Fig. 5) [76]. The ncp sphere array transferred onto the RB:PVA film was pretreated by hot embossing and then used for a mask during RIE process. Sequentially, the substrate with RB:PVA ring-like structured arrays under the SiO_2 arrays was dip-coated in a chloroform solution of PVK with certain concentration. From two-step dewetting behavior, the PVA:RB/PVK heterogeneous double-ring-like structure array was produced on the substrate after removing the sphere arrays.

3-3. Hollow Spheres/Microshells

Using colloidal lithography and metal deposition, various hollow hemispheres such as Pt, Pt/Ag, or Au were successfully generated, extendable to other materials and potential applications such as nanofabrication, nanosensors, and data storage [77,78]. These nanostructures can be generally made by using colloidal arrays as shadow masks. Furthermore, an interesting strategy was simply established to achieve heterogeneous semi-microshells formation on an ncp Si template through stepwise angled colloidal lithography [79]. In addition, for the synthesis of 2D ordered hollow sphere arrays of conductive materials, nonshadow deposition dominated colloidal lithography (NSCL) was demonstrated by Liu and coworkers [80]. They proposed that based on the NSCL strategy, the microstructure of hollow spheres was easily controlled toward more complicated systems (e.g., from single-layer-shell to multilayer-shell, from unitary material to multiple materials, and from simple structure to hierarchically micro/nanostructure).

4. Applications

Various sensing or absorption systems have been developed on colloidal lithographic patterns such as fluorescein-labeled albumin-adsorbed ZnO-SiO_2 nanoplatforms for detection of protein [37], nanoscale E-cadherin ligand or vitronectin patterns for cellular adhesion [81,82], complex protein nanopatterns over large areas [83], and protein-fluorophore binding [84]. Dahlin and coworkers demonstrated a refractometric sensing performance on a metal/dielectric thin film with high aspect ratio holes using "mask-on-metal"

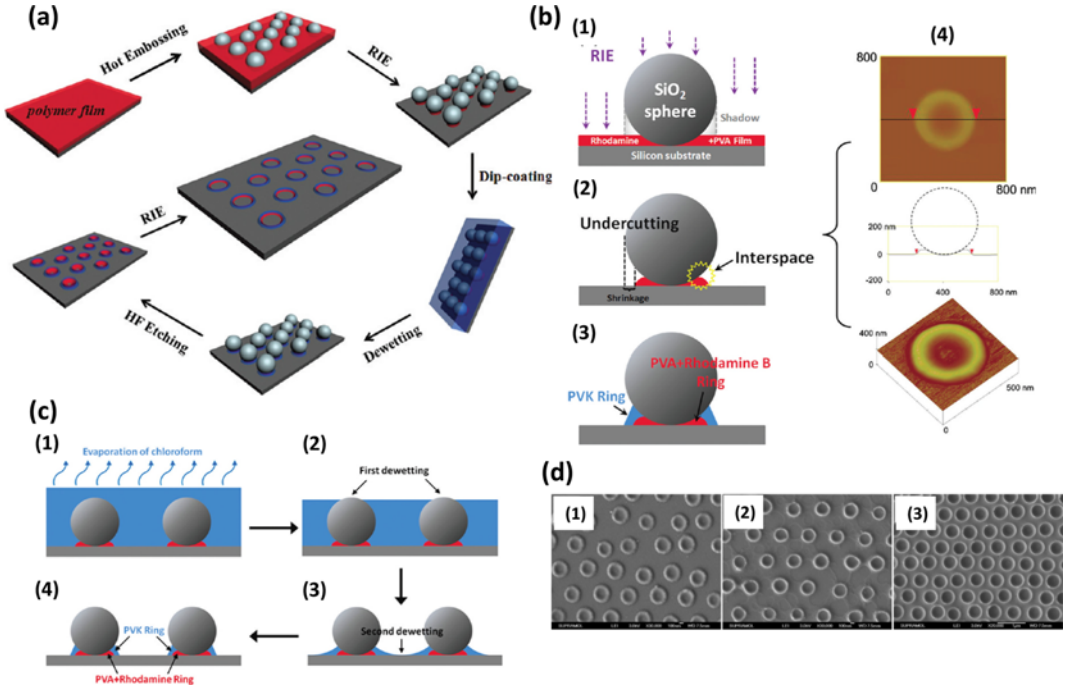

Fig. 5. (a) A procedure for fabrication of ordered heterogeneous double-ring-like (HDR) structure arrays by colloidal lithography and controllable dewetting on a silica substrate, (b) formation process (1-3) and AFM analysis (4) of the HDR structure, (c) a scheme of two-step controllable dewetting process, and (d) SEM images of various morphologies of RB:PVA/PVK HDR structures from different concentrations of PVK solutions [(1) 0.1 mg mL^{-1}, (2) 1 mg mL^{-1}, and (3) 5 mg mL^{-1}]. Reprinted with permission from Ref. 76. Copyright 2013 American Chemical Society.

colloidal lithography and sensing protein (NeutraAdvidin) adsorption inside the nanoholes, so-called "nanowells" [38]. Furthermore, an improved analyte screening method in complex biological matrices was introduced using nanopatterned submicron pores (PEO-pores) as a shield for nonspecific binding in SPR-based sensing [85]. In addition, covalent coupling of protein (BSA) on nano-scaled polydopamine (PDA) patterns in poly-L-lysine-grafted poly(ethylene glycol) (PLL-*g*-PEG) background (protein-repellant region) was employed using bottom-up colloidal lithography, and the attached BSA was recognized by primary/secondary antibodies [86]. In a viewpoint of lipid organizations, fabrication of porous structures based on colloidal lithography was also applied to investigate vesicle adsorption behaviors and a phospholipid bilayer formation on nanostructured Au-SiO_2/SiO_2-SiO_2 [87] or ZnO [88] based porous films.

Moreover, colloidal lithography can be used for optoelectronics devices such as thin solar cells and organic light emitting diodes (OELDs). Using TiO_2 subwavelength surface structures, antireflection and light trapping study was performed on thin film solar cells [89]. The periodic nanoislands formed by colloidal lithography reduced reflectivity through gradient effective refractive indices, whereas they enhanced light trapping due to diffraction in a periodic structure. In addition, Park and coworkers [90] fabricated a perforated WO_3 hole layer to improve light extraction efficiency in OLED. The device showed 60.2% higher power efficiency than a conventional device without the WO_3 layer.

CONCLUSION

The recent development of colloidal lithographic strategies, combined with a bottom-up approach (e.g., the formation of SAMs or polymer brushes) or a top-down approach (evaporation and/or etching process), has led to fantastic 2D nanostructures for analysis, characterization, and applications (sensing systems and optoelectronics, etc). However, despite the great progress chemists/biochemists, physicists, and engineers are still interested in the use of colloidal lithography due to simple methodologies, easy accessibility, and broad applications. To achieve more precise micro-/nanofabrication and optimized nanostructures for further use, there remain more challenges toward the development of advanced lithographic methods and the achievement of new integrated technical progress, extendable their potential for various applications.

ACKNOWLEDGEMENT

This research was supported by Basic Science Research Program through the National Research Foundation of Korea (NRF) funded by the Ministry of Education (NRF-2013R1A1A2061434).

REFERENCES

1. Y. Xia, B. Gates, Y. Yin and Y. Liu, *Adv. Mater.*, **12**, 693 (2000).
2. C. Lopez, *Adv. Mater.*, **15**, 1697 (2003).
3. D. Wang and H. Mchwald, *J. Mater. Chem.*, **14**, 459 (2004).
4. A. Arsenault, S. Fournier-Bidoz, B. Hatton, H. Míguez, N. Tétreault, E. Vekris, S. Wong, S. M. Yang, V. Kitaev and G. A. Ozin, *J. Mater. Chem.*, **14**, 781 (2004).
5. P. Jiang, J. F. Bertone, K. S. Hwang and V. L. Colvin, *Chem. Mater.*, **11**, 2132 (1999).

6. Z.-Z. Gu, A. Fujishima and O. Sato, *Chem. Mater.*, **14**, 760 (2002).
7. D. Wang and H. Mchwald, *Adv. Mater.*, **16**, 244 (2004).
8. P. Jiang and M. J. Mcfarlan, *J. Am. Chem. Soc.*, **127**, 3710 (2005).
9. J. Y. Park, N. R. Hendricks and K. R. Carter, *Langmuir*, **28**(37), 13149 (2012).
10. S. A. Pendergraph, J. Y. Park, N. R. Hendricks, A. J. Crosby and K. R. Carter, *Small*, **9**(18), 3037 (2013).
11. A. van Blaaderen, R. Ruel and P. Wiltzius, *Nature*, **385**, 321 (1997).
12. Y. Yin and Y. Xia, *Adv. Mater.*, **14**, 605 (2002).
13. V. Kitaev and G. A. Ozin, *Adv. Mater.*, **15**, 75 (2003).
14. J. Y. Park and R. C. Advincula, *Soft Matter*, **7**, 9829 (2011).
15. J. Y. Park, P. Dutta and R. Advincula, *Soft Matter*, **7**, 3775 (2011).
16. J. Y. Park, R. Pernites, N. Estillore, T. Hyakutake, R. Ponnapati, B. D. Tiu, H. Nishide and R. C. Advincula, *Chem. Commun.*, **47**, 8871 (2011).
17. F. Sun, W. Cai, Y. Li, B. Cao, F. Lu, G. Duan and L. Zhang, *Adv. Mater.*, **16**, 1116 (2004).
18. P. N. Bartlett, P. R. Birkin, M. A. Ghanem and C.-S. Toh, *J. Mater. Chem.*, **11**, 849 (2001).
19. P. N. Bartlett, J. J. Baumberg, S. Coyleb and M. E. Abdelsalam, *Faraday Discuss.*, **125**, 117 (2004).
20. P. V. Braun and P. Wiltzius, *Nature*, **402**, 603 (1999).
21. J. Zhang, Y. Li, X. Zhang and B. Yang, *Adv. Mater.*, **22**, 4249 (2010).
22. Y. Yu, B. Ai, H. Möhwald, Z. Zhou, G. Zhang and B. Yang, *Chem. Mater.*, **24**, 4549 (2012).
23. S. Giudicatti, A. Valsesia, F. Marabelli, P. Colpo and F. Rossi, *Phys. Status Solidi A*, **207**(4), 935 (2010).
24. T. Chen, I. Amin and R. Jordan, *Chem. Soc. Rev.*, **41**, 3280 (2012).
25. N. Khanduyeva, V. Senkovskyy, T. Beryozkina, M. Horecha, M. Stamm, C. Uhrich, M. Riede, K. Leo and A. Kiriy, *J. Am. Chem. Soc.*, **131**, 153 (2009).
26. R. B. Pernites, E. L. Foster, M. J. L. Felipe, M. Robinson and R. C. Advincula, *Adv. Mater.*, **23**, 1287 (2011).
27. T. Chen, R. Jordan and S. Zauscher, *Soft Matter*, **7**, 5532 (2011).
28. O. Schepelina and I. Zharov, *Langmuir*, **23**, 12704 (2007).
29. N. J. Trujillo, S. H. Baxamusa and K. K. Gleason, *Chem. Mater.*, **21**, 742 (2009).
30. N. J. Trujillo, S. H. Baxamusa and K. K. Gleason, *Thin Solid Films*, **517**, 3615 (2009).
31. A. Dolatshahi-Pirouz, D. S. Sutherland, M. Foss and F. Besenbacher, *Appl. Surf. Sci.*, **257**, 2226 (2011).
32. Y. Kim, R. K. Claus, F. Limanto, R. S. Fearing and R. Maboudian, *Langmuir*, **29**, 8395 (2013).
33. J.-F. Masson, M.-P. Murray-Méthot and L. S. Live, *Analyst*, **135**, 1483 (2010).
34. G. Zhang and D. Wang, *Chem. Asian J.*, **4**, 236 (2009).
35. B. Ai, Y. Yu, H. Möhwald and G. Zhang, *Nanotechnology*, **24**, 035303 (2013).
36. Y.-K. Lin, H.-W. Ting, C.-Y. Wang, S. Gwo, L.-J. Chou, C.-J. Tsai and L.-J. Chen, *Nano Lett.*, **13**, 2723 (2013).
37. C. Satriano, M. E. Fragalá and Y. Aleeva, *J. Colloid Interface Sci.*, **365**, 90 (2012).
38. J. Junesch, T. Sannomiya and A. B. Dahlin, *ACS Nano*, **6**(11), 10405 (2012).
39. M. Yu, Y.-Z. Long, B. Sun and Z. Fan, *Nanoscale*, **4**, 2783 (2012).
40. X. Sun, Y. Li, T. H. Zhang, Y. Ma and Z. Zhang, *Langmuir*, **29**, 7216 (2013).
41. X. Li, T. Wang, J. Zhang, X. Yan, X. Zhang, D. Zhu, W. Li, X. Zhang and B. Yang, *Langmuir*, **26**(4), 2930 (2010).
42. A. Iovan, M. Fischer, R. Lo Conte and V. Korenivski, *Beilstein J. Nanotechnol.*, **3**, 884 (2012).
43. H. Kang, C.-J. Heo, H. C. Jeon, S. Y. Lee and S.-M. Yang, *ACS Appl. Mater. Interfaces*, **5**, 4569 (2013).
44. S. P. Bhawalkar, J. Qian, M. C. Heiber and L. Jia, *Langmuir*, **26**(22), 16662 (2010).
45. J. Qian, S. P. Bhawalkar, Y. Xu and L. Jia, *ACS Appl. Mater. Interfaces*, **2**(11), 3111 (2010).
46. J. H. Park, S. Hwang, B.-K. Kim and J. Kwak, *Electrochem. Commun.*, **30**, 99 (2013).
47. T. Chen, D. P. Chang, R. Jordan and S. Zauscher, *Beilstein J. Nanotechnol.*, **3**, 397 (2012).
48. Y. Li, J. Zhang, W. Liu, D. Li, L. Fang, H. Sun and B. Yang, *ACS Appl. Mater. Interfaces*, **5**, 2126 (2013).
49. K. Chen, J.-J. He, M.-Y. Li and R. LaPierre, *Chin. Phys. Lett.*, **29**(3), 036105 (2012).
50. M.-Y., Li, S. Naureen, N. Shahid and S. Anand, *J. Electrochem. Soc.*, **157**(9), H896 (2010).
51. K. Y. Lai, Y.-R. Lin, H.-P. Wang and J. H. He, *CrystEngComm*, **13**, 1014 (2011).
52. H.-P. Wang, K.-Y. Lai, Y.-R. Lin, C.-A. Lin and J.-H. He, *Langmuir*, **26**(15), 12855 (2010).
53. X. Zhang, J. Zhang, Z. Ren, X. Li, X. Zhang, D. Zhu, T. Wang, T. Tian and B. Yang, *Langmuir*, **25**(13), 7375 (2009).
54. Y. Li, J. Zhang, S. Zhu, H. Dong, F. Jia, Z. Wang, Y. Tang, L. Zhang, S. Zhang and B. Yang, *Langmuir*, **26**(12), 9842 (2010).
55. A. Malainou, K. Ellinas, P. S. Petrou, S. E. Kakabakos, V. Constantoudis, E. Gogolides and A. Tserepi, *Procedia Eng.*, **25**, 1641 (2011).
56. D. H. Lee, Y. Kim, R. S. Fearing and R. Maboudian, *Langmuir*, **27**, 11008 (2011).
57. K. Ellinas, A. Smyrnakis, A. Malainou, A. Tserepi and E. Gogolides, *Microelectron. Eng.*, **88**, 2547 (2011).
58. K. Ellinas, A. Tserepi and E. Gogolides, *Langmuir*, **27**, 3960 (2011).
59. W. Knoben, S. H. Brongersma and M. Crego-Calama, *Nanotechnology*, **22**, 295303 (2011).
60. C. Corbella, S. Portal, M. Rubio-Roy, M. A. Vallvé, J. Ignés-Mullol, E. Bertran and J. L. Andújar, *Diamond Relat. Mater.*, **19**, 1124 (2010).
61. J. R. Oh, J. H. Moon, H. K. Park, J. H. Park, H. Chung, J. Jeong, W. Kim and Y. R. Do, *J. Mater. Chem.*, **20**, 5025 (2010).
62. V. Saracut, M. Giloan, M. Gabor, S. Astilean and C. Farcau, *ACS Appl. Mater. Interfaces*, **5**, 1362 (2013).
63. V. E. Bochenkov, M. Frederiksen and D. S. Sutherland, *Opt. Express*, **21**(12), 14763 (2013).
64. G. Duan, W. Cai, Luo, F. Lv, J. Yang and Y. Li, *Langmuir*, **25**, 2558 (2009).
65. C. Farcau and S. Astilean, *Mater. Lett.*, **65**, 2190 (2011).
66. H. Xu, W. Rao, J. Meng, Y. Shen, C. Jin and X. Wang, *Nanotechnology*, **20**, 465608 (2009).
67. D. Brodoceanu, C. Feng, N. H. Voelcker, C. T. Bauer, A. Wonn, E. Kroner, E. Arzt and T. Kraus, *Nanotechnology*, **24**, 085304 (2013).
68. R. L. Eriksen, A. Pors, J. Dreier, A. C. Simonsen and O. Albrektsen, *Microelectron. Eng.*, **87**, 1471 (2010).
69. B. Wickman, Y. E. Seidel, Z. Jusys, B. Kasemo and R. Jürgen Behm, *ACS Nano*, **5**(4), 2547 (2011).

70. F. Haering, U. Wiedwald, T. Häberle, L. Han, A. Plettl, B. Koslowski and P. Ziemann, *Nanotechnology*, **24**, 055305 (2013).
71. U. Wiedwald, F. Haering, S. Nau, C. Schulze, H. Schletter, D. Makarov, A. Plettl, K. Kuepper, M. Albrecht, J. Boneberg and P. Ziemann, *Beilstein J. Nanotechnol.*, **3**, 831 (2012).
72. A. R. Halpern and R. M. Corn, *ACS Nano*, **7**(2), 1755 (2013).
73. Y. Cai, Y. Li, P. Nordlander and P. S. Cremer, *Nano Lett.*, **12**, 4881 (2012).
74. N. Vogel, J. Fischer, R. Mohammadi, M. Retsch, H.-J. Butt, K. Landfester, C. K. Weiss and M. Kreiter, *Nano Lett.*, **11**, 446 (2011).
75. Z. Li, X. Zhang, S. Ye, J. Zhang, T. Wang, L. Fang, J. Zhang and B. Yang, *Nanotechnology*, **24**, 105307 (2013).
76. D. Zhu, H. Huang, G. Zhang, X. Zhang, X. Li, X. Zhang, T. Wang and B. Yang, *Langmuir*, **28**, 2873 (2012).
77. Z. Chen, J. Fu, Q. Xu, Y. Guo, H. Zhang, J. Chen, J. Zhang, G. Tian and B. Yang, *J. Colloid Interface Sci.*, **391**, 54 (2013).
78. X. Liu, N. C. Linn, C.-H. Sun and P. Jiang, *Phys. Chem. Chem. Phys.*, **12**, 1379 (2010).
79. Y. Yu, L. Gan, G. Zhang and B. Yang, *Colloids Surf., A*, **405**, 51 (2012).
80. G. Duan, F. Lv, W. Cai, Y. Luo, Y. Li and G. Liu, *Langmuir*, **26**(9), 6295 (2010).
81. S. H. Kristensen, G. A. Pedersen, L. N. Nejsum and D. S. Sutherland, *Nano Lett.*, **12**, 2129 (2012).
82. J. Malmström, J. Lovmand, S. Kristensen, M. Sundh, M. Duch and D. S. Sutherland, *Nano Lett.*, **11**, 2264 (2011).
83. S. H. Kristensen, G. A. Pedersen, R. Ogaki, V. Bochenkov, L. N. Nejsum and D. S. Sutherland, *Acta Biomater.*, **9**, 6158 (2013).
84. F. Xie, A. Centeno, M. R. Ryan, D. J. Riley and N. M. Alford, *J. Mater. Chem. B*, **1**, 536 (2013).
85. S. R. Raz, G. R. Marchesini, M. G. E. G. Bremer, P. Colpo, C. P. Garcia, G. Guidetti, W. Norde and F. Rossi, *Analyst*, **137**, 5251 (2012).
86. R. Ogaki, D. T. Bennetsen, I. Bald and M. Foss, *Langmuir*, **28**, 8594 (2012).
87. I. Pfeiffer, S. Petronis, I. Köper, B. Kasemo and M. Zäch, *J. Phys. Chem. B*, **114**, 4623 (2010).
88. C. Satriano and M. E. Fragalà, *RSC Adv.*, **2**, 3607 (2012).
89. P.-C. Tseng, M.-A. Tsai, P. Yu and H.-C. Kuo, *Prog. Photovolt.: Res. Appl.*, **20**, 135 (2012).
90. C. S. Choi, S.-M. Lee, M. S. Lim, K. C. Choi, D. Kim, D. Y. Jeon, Y. Yang and O. O. Park, *Opt. Express*, **20**(S2), A309 (2012).

Jin Young Park is an Assistant Professor in the Department of Polymer Science and Engineering at Kyungpook National University in South Korea. He received Ph.D. degree in the Department of Chemistry from University of Houston, USA in 2009 and worked as a postdoctoral fellow at the University of Massachusetts at Amherst (2009-2012). He was an Assistant Professor at Jungwon University (March 2012-August 2013) before joining Kyungpook National University. His research interests include pi-conjugated polymers, nanomaterials synthesis and nanostructuring, surface science and nanotechnology, molecularly imprinted polymer sensors, electrochemical analysis and synthesis, nanoimprint lithography, and advanced polymer solar cells.